

ELIMINATION OF CYBERNETIC IMPERFECTIONS OF THE FATIGUE TESTING MACHINE

Boris Jerman¹, Janez Kramar¹

¹ University of Ljubljana, Faculty of Mechanical Engineering
1000 Ljubljana, Aškerčeva 6, Slovenia

boris.jerman@fs.uni-lj.si (Boris Jerman)

Abstract

In the production of the elements which are supposed to be subjected to dynamic loading different methods are used for proving their fatigue resistance. One of the most reliable methods is testing of such elements in the laboratories under conditions equal or similar to the real life conditions. For such tests a specially designed large scale testing machines are used which must generally produce a high dynamic loadings at as great frequencies as possible with the aim of ensuring short testing times. Therefore the elements of such machines are subjected to high dynamic loadings too. Besides that also the dynamic properties of the mechanisms used are very important and each imperfection in the design can result in vibrations, additional dynamic loading and in the fatigue of the machine parts. In the paper a design of an existing testing device is presented and the problems in its operation are described. For the solution of the problems the changes in the design of the machine are proposed. Before the application of these changes the proposed solution was confirmed by means of simulations. For this reason a mathematical dynamic model of a machine was developed and the computer program was written for the purpose of numerical integration. After the confirmation the proposed solution was used for enhancement of the design of the problematic machine. The machine is now fully operational and it operates without problems for several years which prove that cybernetic imperfections were eliminated effectively.

Keywords: Fatigue, Testing machines, Dynamic loadings, Numerical models.

Presenting Author's biography

Boris Jerman. He received the M. Sc. and PhD. degrees in Mechanical Engineering from the Faculty of Mechanical Engineering, University of Ljubljana, in 1999 and 2005, respectively. He is currently a teaching assistant at the Faculty of Mechanical Engineering in Ljubljana in fields of steel structures, cranes and other material handling equipment and pressure vessels and a senior lecturer at the Faculty of Chemistry and Chemical technology in Ljubljana in field of Safety of Machinery. His research interests include load carrying structures and non-linear dynamical systems. He is a member of Technical Comities for Cranes and Material Handling Equipment and for Safety of Machinery at Slovenian Institute for Standardization. He is also a member of Slovenian Society of Mechanical Engineers and of Slovenian Society of Occupational Safety Engineers.



$P = 15$ kW at the nominal rotation velocity of $n_N = 1460$ min⁻¹. Nominal moment of the electric motor is $M_n = 700$ N m, the maximal moment is $M_{max} = 2300$ N m and the starting moment of the electric motor is $M_s = 1800$ N m. The rotation velocity of the motor is controlled by means of frequency inverter. The gear of the transmission is $i = 7$ and the nominal rotation velocity of the shaft with the flywheel is $n_1 = 208.6$ min⁻¹ from which the nominal angular velocity $\dot{\varphi} = 3.5$ root/s can be calculated.

The testing specimens are of different heights from $h_{min} = 300$ mm to $h_{max} = 400$ mm. The force - elastic deformation characteristics of the specimens can be linear, progressive or digressive and of the different magnitude. This characteristic must be known as an input data. The force necessary for the elastic deformation of the specimens depends also on the initial settings.

3 The mathematical model

3.1 The special positions of the mechanism

In this section the special positions of the observed mechanism are presented which are important for its mathematical description.

The first special position is the neutral position of the T-beam where the T-beam is in the horizontal position and therefore the angle of the deviation $\psi = 0$ (see Fig. 1 and Fig. 2). Such a position of the T-beam is achieved at two different positions of the crank r , defined by two values of angle φ :

$$\varphi_i = \arcsin \frac{c(r - a \cdot \cos \alpha_i) + (d - b) \cdot a \cdot \sin \alpha_i}{\overline{OB}^2}, \quad (2)$$

$$\overline{OB} = \sqrt{(d - b)^2 + c^2}, \quad (3)$$

$$\alpha_1 = \arccos \frac{a^2 + r^2 - \overline{OB}^2}{2 \cdot a \cdot r} = 76.9^\circ, \quad (4)$$

$$\alpha_2 = 360 - \alpha_1 = 283.1^\circ, \quad (5)$$

$$\varphi_1 = 23.9^\circ, \quad (6)$$

$$\varphi_2 = 211.0^\circ. \quad (7)$$

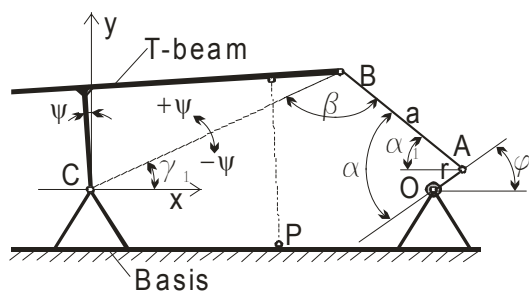


Fig. 2 Key angles of the mechanism

The second special position is the position of the T-beam at the maximal deviation $\psi = \psi_{max}$:

$$\psi_{max} = \arccos \frac{d^2 + R_B^2 - \overline{OB}^2}{2 \cdot d \cdot R_B} - \gamma = 5.7^\circ, \quad (8)$$

$$\overline{OB} = a + r, \quad (9)$$

$$\gamma = \arctg \frac{c}{b} = 27.0^\circ, \quad (10)$$

$$\varphi_3 = 180 - \arccos \frac{d^2 + \overline{OB}^2 - R_B^2}{2 \cdot d \cdot \overline{OB}} = 117.8^\circ. \quad (11)$$

The third special position is the position of the T-beam at minimal deviation $\psi = \psi_{min}$:

$$\psi_{min} = -4.3^\circ, \quad (12)$$

which is calculated by means of Eq.

$$\psi_{max} = \arccos \frac{d^2 + R_B^2 - \overline{OB}^2}{2 \cdot d \cdot R_B} - \gamma = 5.7^\circ, \quad (8) \text{ where:}$$

$$\overline{OB} = a - r, \quad (13)$$

$$\varphi_4 = 360 - \arccos \frac{d^2 + \overline{OB}^2 - R_B^2}{2 \cdot d \cdot \overline{OB}} = 297.9^\circ. \quad (14)$$

The calculated minimal and maximal angles of deviation ψ_{min} and ψ_{max} are discovering the asymmetric nature of the oscillation of the T-beam.

3.2 The mechanism in general position

In this section the equations for the general position of the mechanism are developed. The coordinates of the end point A of the eccentric beam are:

$$x_A = d + r \cdot \cos \varphi, \quad (15)$$

$$y_A = r \cdot \sin \varphi. \quad (16)$$

The coordinates of the point B where the rod a is connected to the T-beam are:

$$x_B = F(\varphi) + G(\varphi) \cdot Y_B, \quad (17)$$

$$y_B = \frac{\Delta h \sqrt{[1 + G^2(\varphi)] \cdot R_B^2 - F^2(\varphi)}}{1 + G^2(\varphi)}, \quad (18)$$

$$F(\varphi) = \frac{R_B^2 a^2 + x_A^2 + y_A^2}{2 \cdot x_A}, \quad (19)$$

$$G(\varphi) = -\frac{y_A}{x_A}. \quad (20)$$

The angles ψ and γ can be calculated:

$$\psi = \arctg \frac{y_B}{x_B} - \gamma, \quad (21)$$

$$\gamma = \arctg \frac{c}{b}. \quad (22)$$

3.3 The kinetic energy of the pendulum

The kinetic energy of the pendulum changes during the swinging motion (changing of the angle ψ). The maximal kinetic energy is identified at the value $\psi = 0$ and $\dot{\psi} = \dot{\psi}_{\max}$:

$$E_{k,\max} = J_{\max} \cdot \frac{\dot{\psi}_{\max}^2}{2}. \quad (23)$$

3.4 The elastic energy of the specimens

The specimens S_1 and S_2 (see Fig. 1) which are tested at the same time must be of the same kind and of the same size. They are elastically deformable for the great extent. Their elastic characteristics can be of the linear, digressive or progressive nature. The specimens are fastened in to the testing machine. When the pendulum (T-beam) is moved from the neutral position the work necessary for this movement is transferred into the potential energy in the form of elastic deformation of the specimens. The maximal potential energy occurs at $\psi = \psi_{\max}$, where the kinetic energy reach its minimum (zero).

The loading moment around the point C , produced by forces F_1 and F_2 which are induced in the elastically deformed specimens S_1 and S_2 can be calculated by formula:

$$M \approx (F_1 - F_2) \cdot x_{Q0}. \quad (24)$$

The elastic forces F_i in specimens S_i are defined by cubic polynomial:

$$F_1 = F_2 = F_0 + c_1 \cdot f + c_2 \cdot f^2 + c_3 \cdot f^3, \quad (25)$$

where F_0 is the initial deformation resistance of the specimen in the case of the neutral position of the T-beam and f is additional deformation of the specimen in the direction of compression or tension of the specimens which occurs when T-beam is declined.

The distortion elastic constant of the pendulum (T-beam + specimens) C_M can be calculated from the elastic loading moment using the following equation:

$$\frac{dM}{d\psi} = \left(\frac{dF_1}{d\psi} - \frac{dF_2}{d\psi} \right) \cdot x_{Q0}. \quad (26)$$

This calculation is included into the developed software.

3.5 The natural frequency of the mechanism

The first natural frequency of the pendulum (T-beam with specimens insulated from the crankshaft r) can be calculated using the known moment of inertia J of the

moving parts and the distortion elastic constant C_M ,

$$\frac{dM}{d\psi} = \left(\frac{dF_1}{d\psi} - \frac{dF_2}{d\psi} \right) \cdot x_{Q0} \quad (26):$$

$$\nu = \frac{1}{2\pi} \cdot \sqrt{\frac{C_M}{J}}. \quad (27)$$

3.6 The differential equation of motion

For detailed analysis of the transient phenomena of starting of the testing machine the Eq.

$$M_M(\dot{\varphi}) - \frac{r \cdot \sin \alpha}{R_B \cdot \sin \beta} \cdot (M_{obr}(\varphi) + J_T \cdot \ddot{\psi}) = (J_M \cdot i^2 + J_{inerc}) \cdot \ddot{\varphi} \quad (28)$$

was written with the reference to the axis O (axis of rotation of the crank r):

$$M_M(\dot{\varphi}) - \frac{r \cdot \sin \alpha}{R_B \cdot \sin \beta} \cdot (M_{obr}(\varphi) + J_T \cdot \ddot{\psi}) = (J_M \cdot i^2 + J_{inerc}) \cdot \ddot{\varphi} \quad (28)$$

where the second derivative of the angle ψ is:

$$\ddot{\psi} = A(\varphi) \cdot \dot{\varphi}^2 + B(\kappa) \cdot \ddot{\varphi}. \quad (29)$$

From the above equations the following differential equation of motion is derived:

$$\ddot{\varphi} = \frac{M_M(\dot{\varphi}) - \frac{r}{R_B} \cdot [M_{obr}(\varphi) + J_T \cdot A(\varphi) \cdot \dot{\varphi}^2] \cdot \frac{\sin \alpha}{\sin \beta}}{J_M \cdot i^2 + J_{inerc} + J_T \cdot B(\varphi) \cdot \frac{r \cdot \sin \alpha}{R_B \cdot \sin \beta}}, \quad (30)$$

The above Eq.

$$\ddot{\varphi} = \frac{M_M(\dot{\varphi}) - \frac{r}{R_B} \cdot [M_{obr}(\varphi) + J_T \cdot A(\varphi) \cdot \dot{\varphi}^2] \cdot \frac{\sin \alpha}{\sin \beta}}{J_M \cdot i^2 + J_{inerc} + J_T \cdot B(\varphi) \cdot \frac{r \cdot \sin \alpha}{R_B \cdot \sin \beta}}, \quad (30)$$

is suitable for the numerical solution. For numerical integration a bespoke computer program was written using Runge-Kutta method and FORTRAN programming language. By this program a fast and accurate calculations were executed providing for the corresponding results.

4 Results

The results obtained from the computer program are in the form of tables. The Excel program is used for graphical presentation of the results. From the graphs so obtained a corresponding size (weight and the dimensions) of the flywheel is chosen and the effectiveness of the proposed solution is demonstrated. For that reason the results are shown for two examples of starting of the testing machine:

- case 1: the original configuration of the machine without the flywheel;
- case 2: the machine is equipped with a new flywheel of the chosen size.

In both cases presented the specimens of the same characteristics are used.

From the Fig. 3 it can be seen that the required power of the driving electric motor during the operation of the testing machine in the case 1 is changing strongly. During the period of acceleration of the system from stand still to the stationary conditions of operation a positive driving moment is developed reaching its maximum value equal to the maximal moment of the motor.

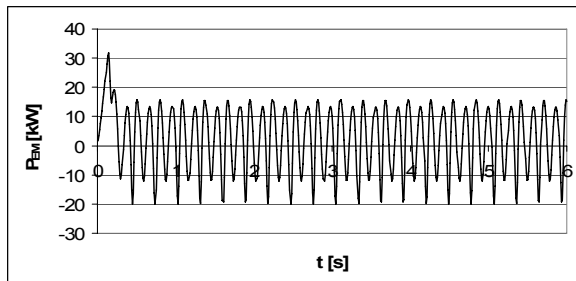


Fig. 3 The required power of the driving motor for the case 1

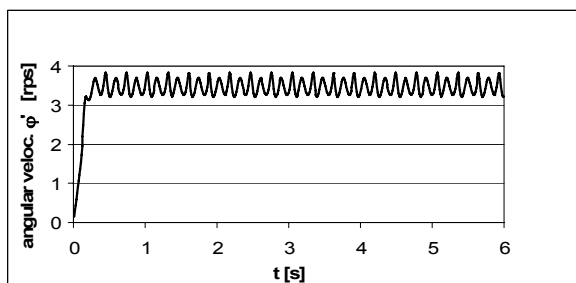


Fig. 4 The angular velocity of the rotation of the crank r for the case 1

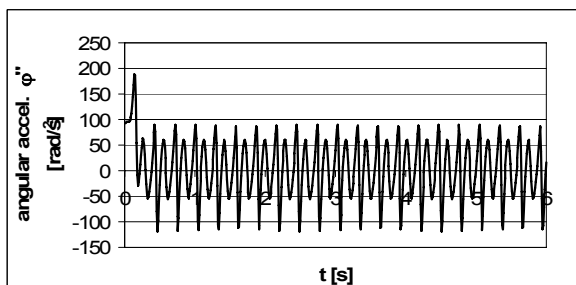


Fig. 5 The angular acceleration of the rotation of the crank r for the case 1

The acceleration phase is ended in less than a quarter of second (see also Fig. 4). After that phase a strong oscillation of the observed moment is encountered in the range from approximately the nominal power of the motor on one hand to the negative value of more than the nominal power on the other hand. That means that the motor is changing the mode of operation from the motor mode to the generator mode and back. In such conditions the control of the motor is almost impossible. The oscillations in the angular velocity of the rotation of the crank are clearly shown on Fig. 4 and strong oscillation of the value of angular acceleration around the average (zero) value is shown on Fig. 5.

Case 2 where the flywheel of an appropriate size is added to the mechanism is introduced by figures Fig. 6 till Fig. 8. On the Fig. 6 the required power during the acceleration is shown. In this case the acceleration phase is much longer than in the case 1 (see also Fig. 7 and Fig. 8) because the driving motor must accelerate the masses of the basic configuration of the mechanism together with the additional mass inertia of the added flywheel. The peak power is again equal to the maximal power of the driving electric motor which is now reached after approximately 2 seconds of operation. After the acceleration phase (near 3 seconds) the oscillation of the needed power is encountered again. The range of oscillations is much smaller than in the case 1 and the electric motor is always in the motor mode of operation which is technically much better than is the situation in the case of the original situation (case 1).

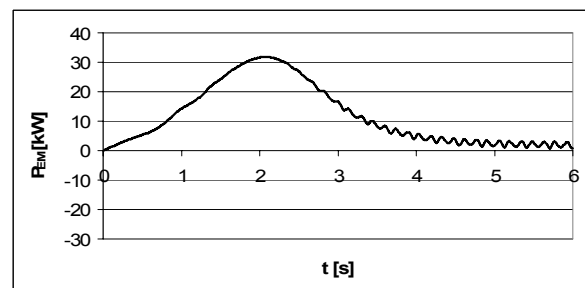


Fig. 6 The required power of the driving motor for the case 2

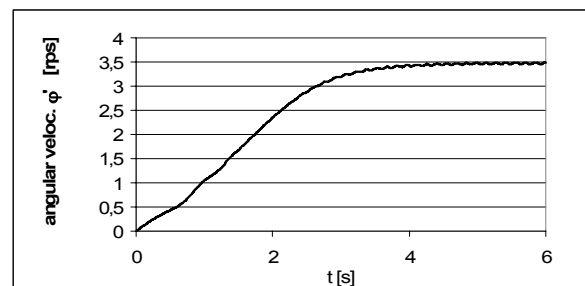


Fig. 7 The angular velocity of the rotation of the crank r for the case 2

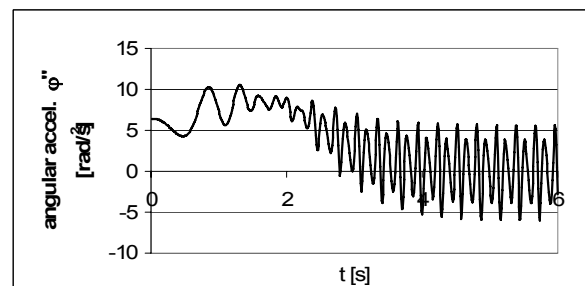


Fig. 8 The angular acceleration of the rotation of the crank r for the case 2

From the Fig. 7 the acceleration time around 3 seconds is estimated and in comparison with the case 1 (Fig. 4) a significantly smaller oscillations of the rotation speed are encountered. The improvement is

demonstrated very clear trough the comparison of the angular accelerations shown on figures Fig. 5 and Fig. 8. The peak values are reduced from approximately $\pm 100 \text{ rad/s}^2$ to approximately $\pm 5 \text{ rad/s}^2$.

In the analysis the friction in the bearings and in the gearbox were not considered because their influences were checked and estimated as no influential and therefore neglect able.

The flywheel with the greater mass moment of inertia would ensure further improvement of the observed dynamic behaviours of the testing machine mechanism. On the other hand this would demand bigger dimensions of the flywheel and also stronger shaft and shaft's bearings which would lead to the necessity of greater changes of the construction of the existing machine and therefore to the greater overall costs of modification. The flywheel of the selected size is convenient also because of the fact that the starting times of the mechanism from zero to the nominal rotation speed remains inside the region from 3 to 4 seconds for all foreseeable cases of usage of the testing machine. This is very important when the heating of the driving electric motor is under the consideration.

Beside the results presented above with the developed software also the internal forces in the individual parts of the observed mechanism can be determined. Because these forces are changing with respect to time a whole loading history for these elements can be predicted which is indispensable for modern fatigue calculations. As an example the force in a connecting rod a is shown in Fig. 9 and force in the crank r in Fig. 10.

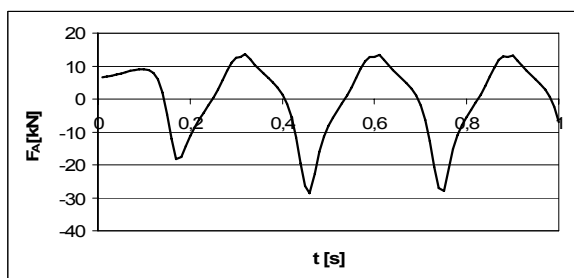


Fig. 9 The force in the connecting rod a for the case 1

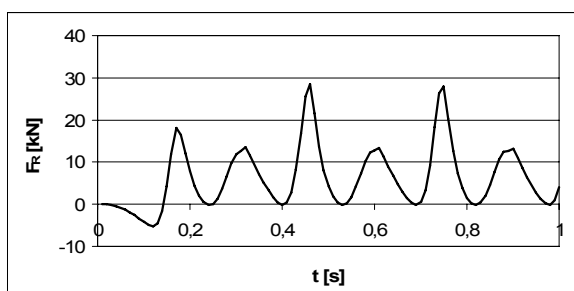


Fig. 10 The force in the crank r for the case 1

4.1 The kinetic energy of the flywheel

The kinetic energy of the flywheel of the selected size in the case of rotation of the driving motor with its nominal angular velocity and is:

$$E_{k, fw} = J_{fw} \cdot \frac{\dot{\varphi}^2}{2}, \quad (31)$$

$$E_{k, fw} = 250 \cdot \frac{21.43^2}{2} = 57405 \text{ J}, \quad (32)$$

This energy is 22.9-times the maximum energy $E_{k, max}$ of the pendulum (see

Eq. $E_{k, max} = J_{max} \cdot \frac{\dot{\psi}_{max}^2}{2}$. (23)) and therefore the

influence of the oscillatory motion on the overall motion of the mechanism is reduced for the great extend.

5 Conclusion

In the paper a usefulness of the mathematical simulations for solution of more complex dynamical problems in the every day's engineer's practice is shown. The idea of building-in an additional flywheel for accumulation of the kinetic energy is analyzed and its efficiency is proven. This idea, of course, represents a classical solution of such dynamical problems but the approach for its realization is fairly original. The correct size of the flywheel is chosen using bespoke software containing newly developed mathematical model, which is presented in the paper. The chosen solution is confirmed by simulations and then applied to the existing machine. The machine now operates without problems which prove that elimination of the imperfections was effective.

6 References

- [1] D. Andersson, A. Petersson, E. Agneholm, D. and Karlsson. Kriegers flak 640 MW off-shore wind power grid connection - A real project case study. IEEE TRANSACTIONS ON ENERGY CONVERSION, 22 (1): 79-85, 2007
- [2] S. I. Kam, Q. P. Nguyen, Q. Li, AND W. R. Rossen. Dynamic simulations with an improved model for foam generation. SPE JOURNAL, 12 (1): 35-48, 2007.
- [3] B. Bienen, M.J. Cassidy. Advances in the three-dimensional fluid-structure-soil interaction analysis of offshore jack-up structures. MAR STRUCT, 19 (2-3): 110-140, 2006.
- [4] N.P. Plakhtienko, B.M. Shifrin. Critical shimmy speed of nonswiveling landing-gear wheels subject to lateral loading. INT APPL MECH, 42 (9): 1077-1084, 2006.